Defluoridation of Morocco drinking water by electrocoagulation/electroflottation in an electrochemical external-loop airlift reactor

M. Bennajah[a,b], B. Gourich[a,*], A.H. Essadki[a], Ch. Vial[c], H. Delmas[b]

[a] *Laboratoire de Génie des Procédés, Ecole Supérieure de Technologie de Casablanca, Km 7 route d'El Jadida, BP 8012, Oasis Casablanca, Morocco*
[b] *Laboratoire de Génie de Procédés, ENSIACET, 118 route de Narbonne, 31077 Toulouse Cedex 04, France*
[c] *Laboratoire de Génie Chimique et Biochimique, Clermont Université, BP 206, 63174 Aubière Cedex, France*

A B S T R A C T

An innovative application of external-loop airlift reactors as electrocoagulation/electroflotation cells with Al electrodes for defluoridation of drinking water was developed. Liquid overall recirculation and mixing were induced only by hydrogen microbubbles electrochemically generated from the cathode. This application was carried out in a 20 L external-loop airlift reactor both under semi-batch and continuous flow conditions. Results showed that liquid recirculation could be correlated to current density and gas–liquid dispersion height in the separator. Experimental data obtained at optimum conditions that favored simultaneously mixing and flotation confirmed that concentrations lower than 1.5 mg/L could be achieved when initial concentrations were between 10 and 20 mg/L. The effects of conductivity and pH agreed with the literature. Conversely, the low electrode surface vs. reactor volume ratio merged the formation of fluoroaluminum microflocs near the electrodes to fluoride adsorption on these particles in the riser and the separator sections, which differed from conventional EC cells. Consequently, defluoridation could be achieved at lower energy and electrode consumptions than in the literature. An optimum current density was defined at $j = 6\ mA/cm^2$ for pH 5, accounting simultaneously for mixing, reaction time, yield and operating costs. A promising attempt of transposition from batch to continuous process was also reported in this work, as flotation avoids the need for a downstream settling unit.

1. Introduction

In drinking water, a minimum fluoride anion concentration is needed to prevent dental cavities, typically higher than 0.5 mg/L, but fluoride content must also remain lower than 1.5 mg/L to avoid dental and skeletal fluorosis [1,2]. The cheapest way to remove fluoride anions consists of the addition of calcium salts (such as lime or calcium chloride), which induces the precipitation of calcium fluorine CaF_2 [3,4]. However, this technique increases the hardness of the water effluents and their fluoride content remains between 10 and 20 mg/L. Alternative methods for defluoridation consist mainly of chemical coagulation using aluminum salts [5], ion exchange [6], adsorption [7–11] and membrane process [12–14]. However, chemical coagulation generates large volumes of sludge and may release secondary pollutants; the adsorption and ion exchange techniques are not able to remove fluoride from water at concentrations higher than 5 mg/L, and the regeneration of adsorbents is costly; the membrane processes are expensive, their efficiency is governed by membrane fouling and requires regular monitoring and maintenance [12–15].

Recent developments have shown that electrocoagulation (EC) constitutes an effective and versatile tool for fluoride removal, both in drinking water and in industrial wastewaters after CaF_2 precipitation [16–20]. It is a process involving the in situ generation of coagulants by dissolving electrically either aluminum or iron ion materials at the anode. Electrolytic gases (typically H_2) are released at the cathode. For aluminum, the main reactions during EC are:

Anode:

$$Al_{(s)}{}^{0} \rightarrow Al^{3+} + 3e^{-}$$

Cathode:

$$2H_2O + 2e^{-} \rightarrow H_{2(g)} + 2OH^{-}$$

Although the sacrificial anodes deliver Al or Fe cations, their dissolution produces hydroxides, oxyhydroxides or polymeric hydroxides as a function of pH [21]. These can adsorb or precipitate

* Corresponding author. Tel.: +212 22 23 15 60; fax: +212 22 25 22 45.
E-mail address: gourich@est-uh2c.ac.ma (B. Gourich).

Nomenclature

A_d	cross-sectional area of the downcomer (m^2)
A_r	cross-sectional area of the riser (m^2)
e	electrode gap (m)
E	specific energy consumption (kWh/kg fluoride removed)
EC	electrocoagulation
EF	electroflotation
F	Faraday's constant (96,487 C/mol e^-)
$[F^-]$	fluoride concentration (mol/m^3)
$[F^-]_0$	initial fluoride concentration (mol/m^3)
g	acceleration of gravity (m^2/s)
h	liquid height in the separator section (m)
h_D	dispersion height in Fig. 1 (m)
$h_{D_{max}}$	maximum dispersion height (m)
H_1	axial position of the electrodes in Fig. 1 (m)
H_2, H_3, H_S	geometrical characteristics of the reactor in Fig. 1 (m)
I	current (A)
j	current density (A/m^2)
K	constant (SI)
K'	kinetic constant ($mol/m^3/s$)
K_B, K_T	friction factors
L, l	electrode length, electrode width (m)
Δm_{exp}	experimental weight loss of Al electrode (kg)
Δm_{th}	theoretical weight loss of Al electrode (kg)
M_{Al}	molar mass of aluminum (0.02698 kg/mol)
P	pressure (Pa)
R	ideal gas constant (J/mol/K)
R^2	correlation coefficient
S	electrode surface area (m^2)
t	time (h)
T	temperature (K)
U	measured potential (V)
U_{Gr}	superficial gas velocity in the riser (cm/s)
U_{Ld}	overall liquid recirculation in the downcomer (cm/s)
U_{Lr}	overall liquid recirculation in the riser (cm/s)
V	reactor volume (m^3)
Y	fluoride removal yield (%)

Greek letters

α	exponent
ε_r	gas hold-up in the riser
ϕ_{Al}	faradic yield of Al dissolution
ϕ_F	efficiency of fluoride adsorption
ϕ_{H_2}	faradic yield of H_2 generation
κ	wastewater conductivity (S/m)
μ_{Al}	specific consumption of the anode (kg Al/kg fluoride removed)
Γ_{max}	maximum of removed fluoride anions per Al^{3+} cations (mol/mol)

both soluble and colloidal polluting species and promote coagulation. Flocs can be removed either by settling followed by filtration, flotation or a combination of these two techniques. In practice, settling is the most common option, while flotation can be achieved by hydrogen or by air injection. Although this technology is known for the 19th Century, the renewed interest in EC stems mainly from its simplicity, environmental compatibility, cost-effectiveness and high efficiency [21]. Indeed, in situ generated coagulants are more effective for pollution removal than added chemicals because they form microflocs that are more likely to flocculate when an electric field is applied, which avoids the use of excessive amounts of chemical coagulants. EC also prevents the presence of co-anions in added chemicals, for example sulphate anions in $Al_2(SO_4)_3{\cdot}18H_2O$ [18] and less sensitive than conventional chemical coagulation to the position of injection points and consequently on mixing conditions. Additionally, EC has been proposed to replace the conventional chemical coagulation because the electrocoagulation process does not require a substantial investment, produces less waste sludge and improves the process efficiency [22].

However, the main deficiency of EC is the lack of dominant reactor design and modelling procedures. Indeed, any systematic approach for design and scale-up was proposed, probably because of the complexity of the interactions between electrochemistry, colloidal forces and hydrodynamics in EC cells. For example, Mollah et al. [23] described six typical configurations for industrial EC cells, but the literature reveals that most EC studies were carried out in laboratory-scale cells in which magnetic stirring was adjusted experimentally to achieve good mixing conditions and for which the separation step by flotation/sedimentation was often disregarded. As a conclusion, the hydrodynamics of the three-phase gas–liquid–solid flow was never investigated, the presence of electrolytic gases being often considered as an unnecessary complication [16].

Another key problem is that fluoride removal by EC is still not fully understood. This stems mainly from the fact that at least three mechanisms compete [20]:

- Adsorption on $Al(OH)_3$ particles:

$$Al_n(OH)_{3n} + m{\cdot}F^- \rightarrow Al_nF_m(OH)_{3n-m} + m{\cdot}OH^-$$

- Coprecipitation:

$$n{\cdot}Al + (3n-m){\cdot}OH^- + m{\cdot}F^- \rightarrow Al_nF_m(OH)_{3n-m}$$

- Fluoride attachment to the electrodes.

The third mechanism is closely linked to coprecipitation because it results simultaneously from the direct coprecipitation of fluoroaluminum compounds on the electrode surface and from the adsorption of colloidal particles of fluoroaluminum complexes formed in the vicinity of the electrode [20]. Actually, the interplay between these three mechanisms depends on many factors, including electrode surface area S, reactor volume V, current density j and water characteristics, which explains why it is still not fully elucidated. In conventional EC cells, the S/V ratio is high, between 10 and 40 m^2/m^3 [16]. Zhu et al. [20] have demonstrated that for $S/V = 18\ m^2/m^3$, attachment to electrodes was primarily responsible for defluoridation efficiency, while other mechanisms exhibited only a secondary effect. Data from the literature showed that direct removal on Al electrodes was promoted by the increase of current density at constant operation time and by higher operation time at constant j, but it decreased with higher $[F^-]_0$ values and in the presence of some co-existing anions [18]. Although Mameri et al. [16] did not discuss the direct attachment of fluoride on electrodes, these authors claimed that fluoride removal was improved when the coprecipitation of fluoroaluminum compounds occurred in the vicinity of the electrodes, which was enhanced by increasing the S/V ratio.

The objective of this work is therefore to demonstrate that airlift reactors can be versatile EC units for defluoridation purpose, which is a key problem in Morocco. Airlift reactors constitute a particular class of bubble columns in which the difference in gas hold-up between two sections (namely the riser and the downcomer) induces an overall liquid circulation without mechanical

agitation. They have been extensively applied in the process industry to carry out both chemical and biochemical slow reactions, but never as EC cells. Airlift reactors present two main designs: external-loop and internal-loop configurations [24]. External-loop airlift reactors offer the advantage to allow various designs of the gas–liquid separator section, which favors gas disengagement at the top of the reactor and maximizes consequently the overall recirculation velocity at the expense of more complex reactor geometries. Their hydrodynamics has also been extensively studied in two-phase gas–liquid and three-phase gas–liquid–solid flows [25]. In this work, the aim is to demonstrate that such reactors can be used as EC cells for defluoridation of drinking water, using only the hydrogen microbubbles electrochemically generated from the cathode (i.e. without air injection) in order to promote good mixing conditions and complete flotation, although they are characterized by low S/V ratios.

2. Materials and methods

2.1. Reactor design

An external-loop airlift made of transparent plexiglas was used (Fig. 1). The diameters of the riser and the downcomer were, respectively, 94 and 50 mm. Both sections were 147 cm height ($H_2 + H_3$) and were connected at the bottom by a junction of 50 mm diameter and at the top by a rectangular gas separator (or gas disengagement section) of H_S = 20 cm height. The distance between the vertical axes of the riser and the downcomer was 675 mm, which limited the recirculation of bubbles and particles from the riser into the downcomer. At the bottom, the curvature radius of the two elbows was 12.5 cm in order to minimize friction and avoid any dead zone. The liquid volume (V) depended on the clear liquid height and could be varied between 14 and 20 L, which corresponded to a clear liquid level (h) between 2 and 14 cm in the separator section. All the experiments were conducted at room temperature (20 ± 1 °C) and atmospheric pressure in both semi-batch and continuous flow modes. Contrary to conventional operation in airlift reactors, no gas phase was sparged at the bottom of the riser; only electrolytic gases (H_2 microbubbles) induced the overall liquid recirculation resulting from the density difference between the fluids in the riser and the downcomer. Two readily available aluminum flat electrodes of rectangular shape (250 mm × 70 mm × 1 mm) were used as the anode and the cathode, which corresponds to S = 175 cm^2 electrode surface area (Fig. 1). The distance between electrodes was e = 20 mm, which is a typical value in EC cells [16]. The electrodes were placed in the riser, parallel to the main flow direction to minimize pressure drop in the riser and maximize the recirculation velocity. The axial position of the electrode could also be varied in the column. The distance (H_1) between the bottom of the electrodes and the bottom of the riser ranged between 7 and 77 cm (Fig. 1). EC was conducted in the intensiostat mode, using a digital DC power supply (Didalab, France) and recording potential during the experiments. The width of the electrodes was maximized by taking into account riser diameter and electrode inter-distance. Electrode length L should be maximized to enhance mixing of dissolved Al and to favor the formation of H_2 microbubbles, but the condition $L < H_2/4$ was retained to avoid limiting the possible H_1 values. As the distance between electrodes was e = 20 mm and the riser diameter 94 mm, it is obvious that a fraction of the liquid phase did not circulate between the electrodes, which did not matter provided residence time in the reactor was far longer than recirculation time and turbulent conditions prevailed in the downcomer. A simple solution would consist in increasing e, but this would reduce electrode surface S at constant L and voltage (i.e. energy requirements) would increase steeply with electrode distance [26]. Current density values (j) between 2.8 and 28 mA/cm^2 were investigated, which corresponded to current ($I = j \cdot S$) in the range 0.5–5 A.

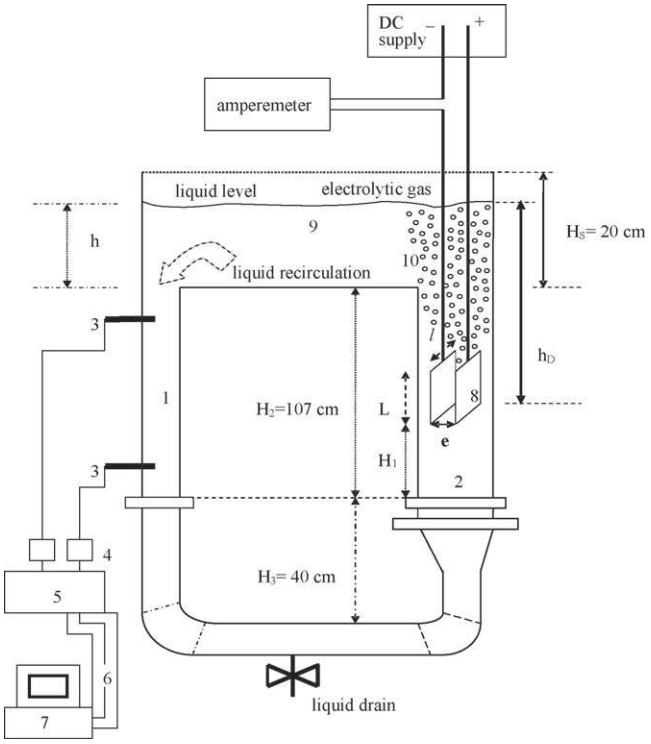

Fig. 1. External-loop airlift reactor (1: downcomer section; 2: riser section; 3: conductivity probes; 4: conductimeter; 5: analog output/input terminal panel (UEI-AC-1585-1); 6: 50-way ribbon cable kit; 7: data acquisition system; 8: electrodes; 9: separator; 10: electrochemically generated bubbles).

2.2. Chemicals and methods

The average liquid velocity in the downcomer (U_{Ld}) was measured using the conductivity tracer technique by means of two conductivity probes placed in the downcomer section in order to record the tracer concentration resulting from the injection of 5 mL of a saturated NaCl solution at the top of the downcomer. The distance between the probes was 90 cm (Fig. 1). The superficial liquid velocity in the riser (U_{Lr}) was deduced from a mass balance on the liquid phase:

$$U_{Lr} = U_{Ld}\frac{A_d}{A_r} \quad (1)$$

in which A_r and A_d are the cross-sectional area of the riser and the downcomer, respectively.

Experiments were carried out using typical Casablanca drinking water (Table 1) in which an initial fluoride concentration $[F^-]_0$ between 10 and 20 mg/L was obtained by adding sodium fluoride NaF (Carlo Erba Réactifs, France). Electrocoagulation time was 35 min, except when longer time was required to achieve the objec-

Table 1
Tap water properties

pH	7.85
Alkalinity (°f)	15
Total hardness (°f)	35
Turbidity (NTU)	0.15
Conductivity (μS)	1600 (20 °C)
Chloride [Cl^-] (mg/L)	392

tive of 1.5 mg/L fluoride. Water conductivity and pH were measured on filtered samples using a CD810 conductimeter (Radiometer Analytical, France) and a ProfilLine pH197i pHmeter (WTW, Germany), respectively. Experimental values reported in this work correspond to the average of two samples. Fluoride concentration [F^-] was measured by means of a fluoride-selective combined electrode (ISEC301F^-) and a PhM240 ion-meter (Radiometer Analytical, France), using the addition of a TISAB II buffer solution to prevent interference from other ions. The water conductivity κ (2.1 mS/cm) could be increased up to 21 mS/cm by the addition of sodium chloride NaCl. This is quite common in EC processes, as NaCl plays the role of supporting electrolyte and prevents electrode passivation, while presenting the advantages to be non-toxic and of reasonable cost. This addition had a negligible effect on the initial pH of the solutions and pH could be adjusted by minute addition of either HCl or NaOH aqueous solutions. The effectiveness of fluoride removal was quantified by the removal yield Y, defined as the ratio of fluoride removed over the initial amount of fluoride in water:

$$Y\,(\%) = \frac{[F^-]_0 - [F^-]}{[F^-]_0} \times 100 \quad (2)$$

The evolution of turbidity over time was measured on non-filtered samples in order to follow whether the flocs floated or were destroyed and driven by the liquid flow using a 550IR turbidimeter (WTW, Germany). As for pH, conductivity and fluoride concentration, samples were recovered in duplicate from the liquid drain in batch process, and from and the effluent stream under steady state operation. The specific electrical energy consumption (E) and the specific electrode consumption (μ_{Al}) to achieve the desired Y value were calculated as follows:

$$E\,(\mathrm{kWh/kg\,F^-}) = \frac{UI \cdot t}{VY \cdot [F^-]_0} \quad (3)$$

$$\mu_{Al}\,(\mathrm{kg\,Al/kg\,F^-}) = \frac{\phi_{Al}\, M_{Al} \cdot I \cdot t}{3F \cdot VY \cdot [F^-]_0} \quad (4)$$

using cell voltage U, electrolysis time t, molar weight of aluminum M_{Al}, Faraday's constant F and the faradic yield ϕ_{Al} of Al dissolution. ϕ_{Al} was estimated as the ratio of the experimental weight loss of the Al electrodes Δm_{exp} and the amount of aluminum consumed theoretically at the anode deduced from Faraday's law Δm_{th}:

$$\phi_{Al} = \frac{\Delta m_{exp}}{\Delta m_{th}} = \frac{3F}{M_{Al} \cdot I \cdot t} \cdot \Delta m_{exp} \quad (5)$$

For weight loss measurements, electrodes were washed using a dilute HCl solution in order to remove deposits and dried before weighing in triplicate. The deviation of the weight loss from the Faraday's law was between $30 \pm 5\%$ and $60 \pm 5\%$. At the end of EC, sludge was recovered, dried and observed using scanning electron microscopy equipped with an EDX detector that gave access to the chemical composition of sludge, especially to the F/Al ratio.

3. Experimental results on hydrodynamics

Experimental results highlighted that reactor hydrodynamics was governed by two key parameters: namely the current density (j) and the gas–liquid dispersion height (h_D) where h_D results from the axial position of the electrodes H_1 in the riser and the clear liquid height in the separator (h). Other parameters, such as conductivity and pH, did not change significantly the overall liquid recirculation velocity. Bubble recirculation in the downcomer was never observed, probably because of the low liquid velocities, even when h was 2 cm, which confirmed that gas flow rate due to electrochemically generated H_2 microbubbles was far lower than in conventional airlift applications. The same stands for bubble diameters that ranged between 50 and 100 m, far smaller than sparged air bubbles even in non-coalescing media, with a flotation speed estimated from Stokes law between 1 and 5 mm/s. As a result, only the gas hold-up in the riser ε_r will be considered. ε_r is defined as the gas volume fraction in the aerated region of the riser; however, ε_r values could not be estimated precisely in this work because they were too low to be measured experimentally. This means that the dispersion height could not be distinguished from the clear liquid height. Indeed, using Faraday's law, the superficial gas velocity in the riser U_{Gr} could be estimated using:

$$U_{Gr} = \frac{1}{A_r} \cdot \frac{\phi_{H_2} I}{2F} \cdot \frac{RT}{P} \quad (6)$$

in which ϕ_{H_2} is the faradic yield of H_2 generation, T is the operation temperature and P is atmospheric pressure. Even using $\phi_{H_2} = 2.2$, the highest value reported by Khemis et al. [27], U_{Gr} values were always lower than 1 mm/s in this work. Using the correlations from the literature on airlift reactors [24], ε_r should be negligible. Nevertheless, these correlations do not consider the case of electrochemically generated microbubbles with a low slip velocity, which increased their residence time in the riser. As a result, ε_r was weak in the riser, but far higher than predictions obtained from classical correlations available for airlift reactors [24].

Measurements of the liquid recirculation velocity in the downcomer U_{Ld} for h = 14 cm are reported in Fig. 2 for two axial positions of the electrodes that correspond roughly to the bottom (H_1 = 7 cm) and the middle (H_1 = 47 cm) of the riser as a function of j. For H_1 > 77 cm, i.e. when the electrode position approached the top of the riser, liquid recirculation vanished. Due to the low velocity values and the high residence time in the gas–liquid separator section, measurements of mixing time and circulation time were not precise enough to be reported, although these quantities are directly linked to the superficial liquid velocity. On the other hand, turbidity measurements in the downcomer showed that complete flotation was achieved only when H_1 > 56 cm, regardless of j, in the range studied when h was 14 cm. This confirmed that flocs break-up or erosion did not occur when U_{Ld} was lower than 4–5 cm/s. A comparison with a previous work on the decolorization of textile dye wastewater in the same setup [28] shows two interesting points: U_{Ld} vs. j values were similar for both waters, but floc erosion could be avoided when U_{Ld} was lower than 8–9 cm/s in the presence of dispersive dyes, which provided a larger range of H_1 values for Essadki et al. [28]. This demonstrates that U_{Ld} seems nearly independent of the nature of soluble polluting species, but that floc stability may strongly vary with pollutants and other compounds in water, such as dissolved salts or colloids. As a result, Al electrodes were placed at a distance

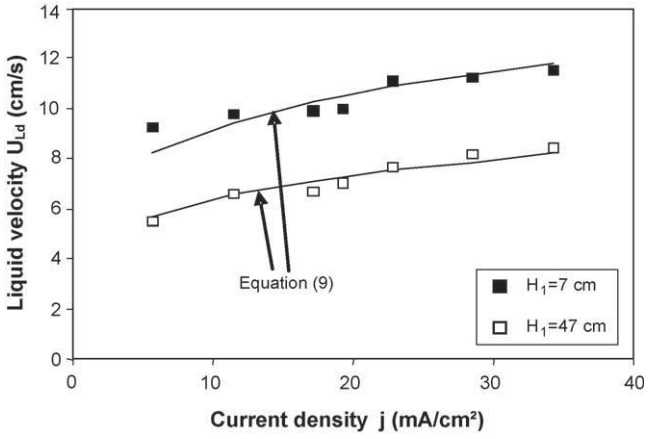

Fig. 2. Influence of the axial position of the electrodes (H_1) and of current density (j) on the overall liquid recirculation U_{Ld} (h = 14 cm; initial pH: 7; [F^-]$_0$ = 15 mg/L).

H_1 = 58 cm from the bottom of the riser in this work, which maximized the overall liquid recirculation velocity. This ensured that turbulent conditions just prevailed in the downcomer, which was necessary to achieve good mixing conditions, as the gap between electrodes was lower than riser diameter in order to reduce voltage and therefore energy supply.

A model based on Chisti's equation [24,29] was developed to correlate U_{Ld}, h_D and j. When gas hold-up in the downcomer is negligible, the energy balance model reduces to:

$$U_{Lr} = U_{Ld}\frac{A_d}{A_r} = (2gh_D\varepsilon_r)^{0.5} \cdot \left[K_T(1-\varepsilon_r)^{-2} + K_B\left(\frac{A_r}{A_d}\right)^2\right]^{-0.5} \quad (7)$$

in which h_D corresponds to the dispersion height, while K_T and K_B account, respectively, for the effects of pressure drop in the riser and in the downcomer. This expression could be modified to take into account that only a fraction of the riser was aerated with $\varepsilon_r \ll 1$ and that the friction factor was nearly constant:

$$U_{Ld} = K \cdot (\varepsilon_r h_D)^{0.5} \quad (8)$$

where h_D is the distance from the surface for which a gas phase can be observed in the riser (Fig. 1) and K is a constant. As mentioned above, at constant H_1, h_D should be nearly independent of gas flow rate when $\varepsilon_r \ll 1$. On the basis of empirical correlations from the literature [25], ε_r should vary with superficial gas velocity U_{Gr} as U_{Gr}^{α} with α between 0.5 and 0.6 in external-loop airlift reactors. As gas flow rate should be proportional to current, this gives $U_{Ld} \sim I^{\alpha/2}$. Experimental data was fitted for each H_1 value as a function of j using the Levenberg–Marquardt algorithm. The optimization procedure lead to $\alpha = 0.4 \pm 0.02$. Using data at $h_{D_{max}}$ as a reference ($h_{D_{max}}$ is the maximum dispersion height corresponding to H_1 = 7 cm), the influence of H_1 was expressed through the ratio $h_D/h_{D_{max}}$. The optimization procedure using experimental data lead to a simplified model with $U_{Ld} \sim (h_D/h_{D_{max}})^{0.6\pm0.1}$ The small range of h_D values available in this work was probably responsible for the larger error on the exponent estimation. One found finally:

$$U_{Ld} = 3.7 \cdot 10^{-2} \cdot \left(\frac{h_D}{h_{D_{max}}}\right)^{0.6} \cdot j^{0.20} \quad (9)$$

The good agreement between predictions and experiments is illustrated in Fig. 2. The fitted parameter α = 0.40 was a bit lower than expected from theoretical considerations, but this result is however satisfactory if one considers that the correlations used for comparison are based on U_{Gr} values far higher than those of this work.

Dispersion height h_D could also be modified by varying the clear liquid height in the gas–liquid separator section (h). Experimental results at constant H_1 confirmed the validity of Eq. (9). The influence of h on h_D in the range studied (between 2 and 14 cm) was however far weaker than that of H_1, about ±10% of U_{Ld} values. Nevertheless, low h values could lead to particle recirculation in the downcomer, which had to be avoided. For instance, when h was equal to 2 cm, the sludge occupied almost the total volume of the disengagement section, allowing the flocs to be driven by the liquid flow. As far as h was increased, the flotation layer thickness at the surface occupied a decreasing volume fraction of the disengagement section, which limited floc break-up and erosion in the separator. Finally, complete flotation without floc recirculation was achieved when h was higher than 6 cm, probably because of the large distance between the riser and the downcomer. Experimental data, not reported, is similar to that of Essadki et al. [28] for decolorization in the same airlift reactor.

As a conclusion, liquid recirculation with good mixing conditions and complete flotation could be achieved using only the electrochemically generated microbubbles, provided the Al electrodes were adequately placed in riser. The clear liquid height could be used to adjust precisely the desired velocity, but h presents a minimum value in order to obtain complete flotation conditions. In this work, H_1 = 58 cm and h = 14 cm were retained, which allowed to work with U_{Lr} about 1.5 cm/s. Using this value, a rough estimation of the minimum circulation time that could be achieved was less than 3 min. As mixing time in external-loop airlift reactors is known to be about five circulation times [30,31], the EC time retained, 35 min, corresponded roughly to 12 circulation time and was high enough to maintain adequate mixing conditions. The above results justify also the choice of an external-loop airlift reactor because its geometry permits large distances between riser and downcomer in order to favor complete flotation, which is not possible in internal-loop airlift reactors.

4. Application to defluoridation

4.1. Efficiency of batch treatment

The objective was to achieve final [F^-] values lower than 1.5 mg/L. Using the optimized position of the electrode defined in Section 3 (H_1 = 58 cm and h = 14 cm), the respective influences of the operating conditions of EC (such as current density, operation time, initial fluoride concentration $[F^-]_0$) and of the physicochemical properties of water before treatment (such as initial pH and conductivity) were investigated in order to achieve the objectives by complete flotation. For all the defluoridation experiments reported below, complete flotation was always observed with H_1 = 58 cm and h = 14 cm. Indeed, turbidity values remained low in the downcomer, which confirmed that the flocs were stable over time. ϕ_{Al} was always between 1.3 and 1.6; it decreased when operation time and current density were increased, which is in agreement with the literature [27,28]. This mass overconsumption of aluminum electrodes has often been attributed to the chemical hydrolysis of the cathode that is increased by corrosion pitting phenomenon in the presence of chloride anions.

In the airlift reactor of this work, the S/V ratio was far lower (0.875 m^2/m^3) than in a conventional EC cell, which should favor the mechanisms that involve the bulk, i.e. purely chemical coprecipitation or, more likely, adsorption, according to Mameri et al. [16]. Indeed, EC in the airlift reactor differs significantly from conventional EC cells:

- Experimental results show that increasing j at constant $[F^-]_0$ values modified only slightly defluoridation above 5.7 mA/cm^2 and the effect became negligible above 8.6 mA/cm^2 during the first 15 min. Such a phenomenon had already been reported by Mameri et al. [16], but for current density above 20 mA/cm^2 for S/V = 6.9 m^2/m^3, and it was reported to stem from the fact that adsorption in the bulk became the limiting step.
- At constant current density (j = 17 mA/cm^2) and various $[F^-]_0$ values, a zero-order kinetics was observed in the airlift reactor (Fig. 4), whereas conventional EC follows usually first-order kinetics [16,32]. Additionally, the slope corresponding to the zero-order mechanism in Fig. 4 was nearly independent of $[F^-]_0$.

However, if a purely chemical coprecipitation mechanism followed by adsorption played the key role, the results of Figs. 3 and 4 would be similar to a chemical coagulation operation. This assumption must be rejected, first because EC has always been reported to be more efficient than chemical coagulation for defluoridation (see Section 1), but also because the airlift reactor is more efficient than conventional EC cells to carry out fluoride removal. For example,

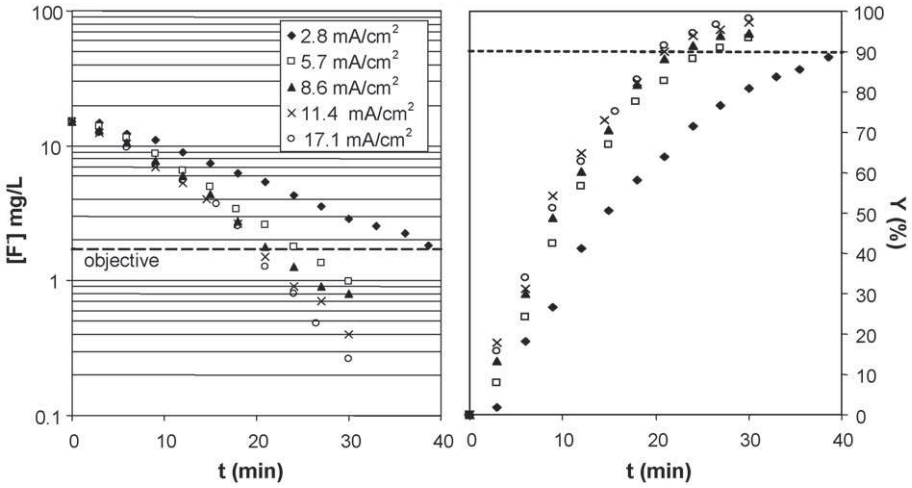

Fig. 3. Influence of j on F^- removal (initial pH 7; $[F^-]_0 = 15$ mg/L).

a comparison with the data of Emamjomeh and Sivakumar [32] shows that the need for dissolved Al cations was far lower in the airlift reactor: 25 min operation at 50 A/m^3 water were required in this work for $j = 5.7$ mA/cm^2, while these authors needed between 30 and 60 min and between 273 and 683 A/m^3 for similar initial pH and initial fluoride concentration to achieve 1.5 mg/L. Similarly, a comparison with the data of Shen et al. [19] shows that they required 5–6 Faradays/m^3 to achieve 1.5 mg/L with $[F^-]_0$ between 10 and 15 mg/L, while this work needed 1.5–3 F/m^3 for the same objective. Finally, a comparison of the F/Al mass ratio of the sludge in this work with the data of Hu et al. [18] for the closest operating conditions (pH, fluoride initial concentration and co-anions) shows that their value was about 0.15, while it was about 0.2 in the airlift reactor after 35 min operation for nearly the same fluoride removal efficiency. As a result, the above-mentioned considerations demonstrate clearly that EC in the airlift reactor is neither limited by the formation of fluoroaluminum complexes near the electrodes, as in conventional EC cells [16,18], nor by the purely chemical coprecipitation of $Al_n(OH)_{3n}$ followed by adsorption in classical coagulation operation.

Actually, defluoridation in the airlift reactor seems to take benefits from the electrogeneration of fluoroaluminum complexes, as in conventional EC cells. Indeed, in situ generated coagulants are more effective for pollution removal than added chemicals because they form microflocs that are more likely to flocculate when an electric field is applied. In the airlift reactor, electrodes generate highly active fluoroaluminum microflocs, but locally. Then, in the riser and the separator sections, these microflocs can adsorb additional fluoride anions without energy and Al requirements. The fact that adsorption may be the limiting step near the electrodes is counterbalanced by the long residence time of the particles in the riser and the separator. Finally, the low S/V ratio enhances fluoride removal in the bulk on already formed fluoroaluminum solid particles, which requires no additional current and consequently less power than the electrochemically driven coprecipitation of fluoroaluminum compounds on or at the vicinity of the electrode surface in conventional EC cells. Additionally, no mechanical mixing is required in the airlift reactor. As a result, power requirements should be lower in the airlift reactor. This will be confirmed quantitatively in the next section.

The role of adsorption far from the electrodes as a mechanism complementary to the electrogeneration of fluoroaluminum complexes for fluoride removal is particularly corroborated by the zero-order kinetics of Fig. 4. In the literature, this kind of kinetics may be analyzed in relation to a model developed by Hu et al. [33]. This assumes a F^- adsorption mechanism based on a Langmuir isotherm and corresponds to a variable-order kinetics that is zero-order at high fluoride concentration with a kinetic constant K'

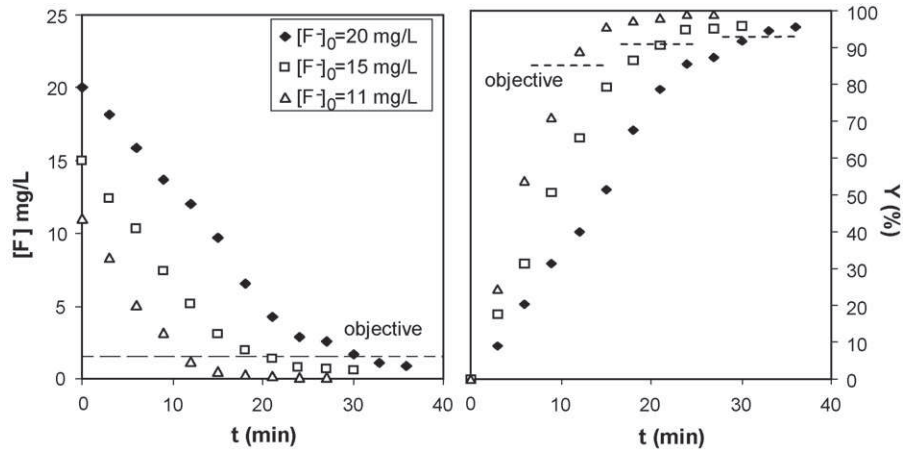

Fig. 4. Influence of $[F^-]_0$ on F^- removal (initial pH 7; current density: $j = 17$ mA/cm^2).

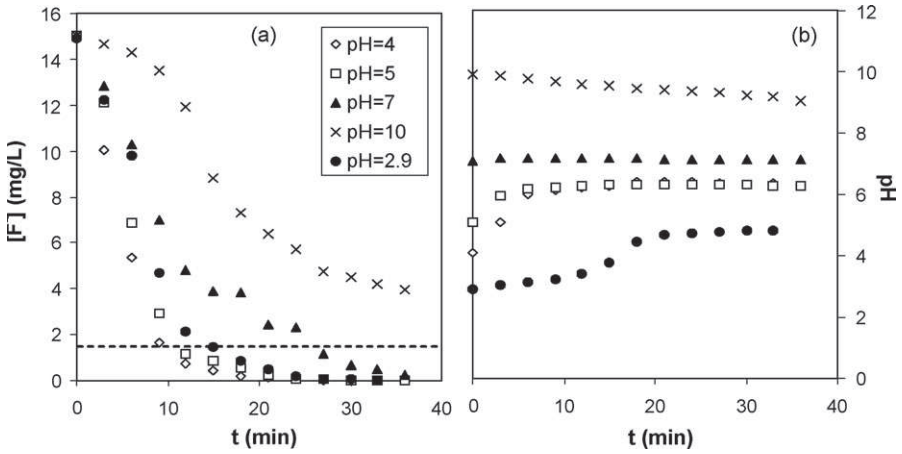

Fig. 5. Influence of initial pH on F^- removal (a) and pH evolution with time (b) ($[F^-]_0$ = 15 mg/L; current density: j = 17 mA/cm^2).

equal to:

$$K' = \phi_{Al}\phi_F \frac{I}{3FV}\Gamma_{max} \quad (10)$$

in which ϕ_F is the efficiency of fluoride adsorption and Γ_{max} the maximum of removed fluoride anions per Al^{3+} cations (mol/mol). Conversely, the kinetics tends to be first-order at low $[F^-]$ values. In Fig. 4, the slope of the linear region is about 0.75 ± 0.05 mg L^{-1} min^{-1} for I = 3 A, regardless of $[F^-]_0$. A comparison with the theoretical values of Hu et al. [33] cannot be straightforward because the range of initial pH used by these authors differs from that of this work, but it gives K' between 0.4 and 0.7 mg L^{-1} min^{-1} using Γ_{max} between 0.55 and 0.81 and ϕ_F between 0.86 and 1, which is in fair agreement with our data.

As a result, the decrease of removal efficiency due to the small S/V ratio that could be expected in the airlift reactor is overshadowed by two main mechanisms:

- The above-mentioned zero-order kinetics that maintains the minimum necessary time for F^- removal in order to achieve 1.5 mg L^{-1} or less residual fluoride in the effluents.
- The recirculation in the loop with a circulation time a bit lower than 3 min (which means that water is treated about 12 times in 35 min) and the complete separation of the flocs by flotation in the separator section at each recirculation.

Finally, all these results and analyses confirm that EC reactors with low S/V ratios are adequate tools for defluoridation because they favor F^- removal in the bulk on electrogenerated fluoroaluminum complexes, which is less mass- and energy-consuming than the direct electrochemical fluoride removal on or in the vicinity of electrodes located everywhere in the reactor.

Conversely, fluoride removal by direct attachment on electrodes should play only a secondary role in the airlift reactor due to the low S/V ratio. The reduction of the influence of this mechanism can be roughly quantified. For Zhu et al. [20], it could contribute up to 80% of the efficiency of fluoride removal in conventional EC cells. Although electrode material is not exactly the same, the maximum fluoride anion adsorbed on electrodes in the work of [20] was 0.05 mg/m^2 electrode. Using the S, V and initial concentration values of our work, electrodes could remove only 0.5 mg/L fluoride anion for $[F^-]_0$ between 10 and 20 mg/L in the airlift reactor. Direct attachment on electrodes and coprecipitation near the electrodes can however explain the change of the kinetics of fluoride removal in the airlift reactor observed for j > 6 mA/cm^2 when $[F^-]$ was lower than 3 mg/L (Fig. 3). Similarly, defluoridation is probably limited by the coprecipitation of fluoroaluminum complexes near the electrodes when j < 6 mA/cm^2 (Fig. 3). These behaviors may therefore be interpreted as transitions characterizing a change of the mechanism governing defluoridation.

Contrary to current and $[F^-]_0$, the effects of pH and conductivity agreed with the literature on EC. The influence of the initial pH is reported in Fig. 5a. pH varied also with time during EC and could either increase or decrease as a function of the initial pH value (Fig. 5b). Experiments up to initial pH 7 lead to a pH increase, but when initial pH higher than 8, pH exhibited a decrease vs. time. This confirms the results of Mameri et al. [16] who found that EC exhibited a buffering effect and that pH tended towards 7.6, where the fluoroaluminum complexes present the maximum stability. In this work, the optimum initial pH was between 4 and 5.2, which agreed qualitatively with the data of Hu et al. [33]. Similarly, Mameri et al. [16] found that optimum initial pH was around 5. The influence of water conductivity is illustrated by Fig. 6a. An increase of κ by NaCl addition favored F^- removal. This behavior has been often observed in the literature on EC and can be attributed to the effect of chloride anions that prevent electrode passivation and avoid the precipitation of carbonates [16]. Another advantage is that voltage, i.e. power requirements, decrease when κ increases at fixed j. Voltage is linked to current density by the model developed by Chen et al. [26] for non-passivated flat electrode (Eq. (11)) that fits very well experimental data up to 20 mA/cm^2 (Fig. 6b), regardless of $[F^-]_0$ and pH.

$$U = -0.76 + \frac{e}{\kappa} j + 0.20 \cdot \ln(j) \quad (11)$$

One should note that this equation takes also into account the effect of electrode gap e. However, an excessive amount of NaCl (higher than 3 g/L) is known to induce overconsumption of the aluminum electrodes due to corrosion pitting and Al dissolution may become irregular [34]. Additionally, high chloride content exceeds usually the maximum concentration tolerated in waters destined to human consumption. As a conclusion, κ about 5 mS/cm seems a reasonable compromise because it offers a moderate value of electrical consumption by Joule effect, while preventing a rapid degradation of the electrode surface.

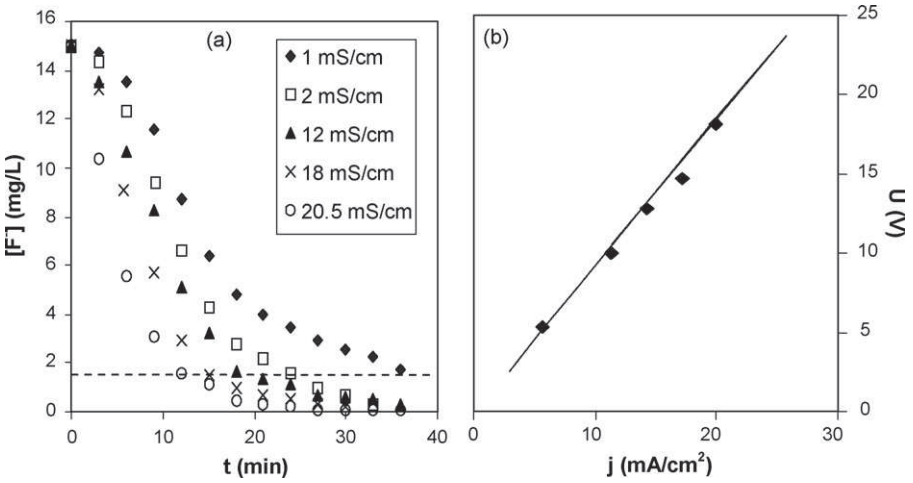

Fig. 6. Influence of κ on F^- removal (a) at pH 7 and $j = 17\ mA/cm^2$, and of current density j on voltage U (b).

4.2. Energy consumption and cost

In order to optimize EC, two parameters must be taken into account: the cost of the sacrificial anode and that of energy supply. The E and μ_{Al} specific parameters (Eqs. (3) and (4)) calculated at the minimum time required to achieve the objective of 1.5 mg/L can be used to estimate both. They are illustrated in Fig. 7 for $[F^-]_0 = 15$ mg/L without NaCl addition, both as a function of initial pH and j. Energy costs increased continuously as a function of current density (Fig. 7a) because the decrease of the time necessary to achieve fluoride removal (Fig. 3) did not compensate the increase of power supply that varied roughly as $j^{1.5}$. On the other hand, μ_{Al} was nearly constant between 2 and 6 mA/cm^2. This could be attributed to a decrease of EC effectiveness at low j values, but also to the reduction of the overall liquid velocity and of the mixing efficiency in the reactor (Eq. (9)). Power requirements could also be reduced by increasing water conductivity, which varied roughly as $1/\kappa$, but this increase is limited and the additional cost of NaCl should also be taken into account. pH adjustment around 5 seems therefore cheaper and more effective (Fig. 7b). As 1 kg electrode material is about 30 times more expensive than 1 kWh electricity, one can consider that pH 5 and $j = 6\ mA/cm^2$ correspond to the optimum conditions. Indeed, the need for initial pH change is minimum and this current density gives reasonable reaction times and U_{Ld} values around 4–5 cm/s (Fig. 2), which is enough to maintain adequate mixing conditions in the reactor. Additionally, the adjustment of initial pH is easy because the amount of buffering species in drinking water is usually weak and final pH is above 6 (Fig. 5b) due to the buffering effect of EC process, which avoids the need for downstream pH adjustment. As a rule of thumb, EC requires 1 kg aluminum per kg fluoride to achieve the objective in 10 min at initial pH between 4 and 5, which is not much if one considers both the toxicity of fluoride and the low fluoride content to remove from water (lower than 20 mg/L). This value agrees with the F/Al mass ratio in the flocs recovered for the conditions at the end of EC time, 35 min, which is about 0.32. Indeed, additional Al released from the electrodes should first eliminate the residual fluoride concentration (Fig. 5) and then dilute fluoride in the flocs: calculations based on $[F^-] = 1.5$ mg/L and $F/Al \approx 1$ after 10 min EC give an estimated F/Al value about 0.3 with the assumption $[F^-] = 0$ after 35 min EC, which matches perfectly the experimental value.

4.3. Transposition to continuous operation

For water distribution, the batch mode operation is usually of little usage. However, it constituted a necessary step, as defluoridation in airlift reactors had never been reported up to now. As U_{Ld} was a weak function of j (Eq. (9)), circulation and mixing times could be assumed to be nearly constant, with a circulation time about 3 min. The net liquid flow rate was fixed at 1 L/min with a liquid injection point in the junction at the bottom of the riser, while the effluent stream was recovered from the junction at the bottom of the downcomer. The net flow rate corresponded to a residence time of 20 min, which is higher than five circulation times. Additionally, this value

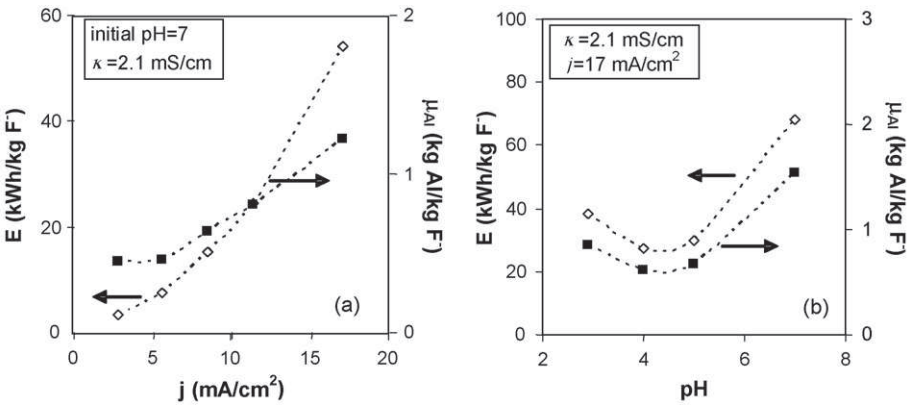

Fig. 7. Evolutions of specific energy (E) and electrode (μ_{Al}) consumptions vs. j and pH ($[F^-]_0 = 15$ mg/L) based on the minimum time to achieve the objective ($[F^-] = 1.5$ mg/L).

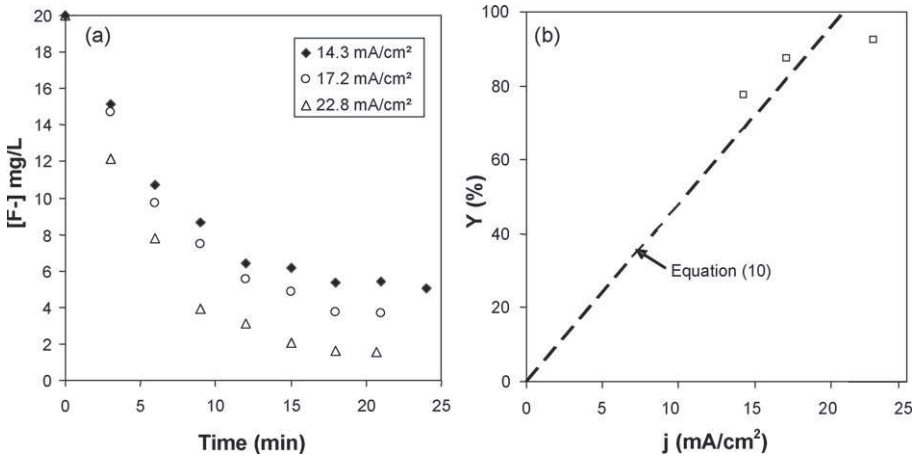

Fig. 8. Experimental results of continuous defluoridation process (pH 7, $[F^-]_0 = 20$ mg/L): (a) study of the establishment of steady state conditions; (b) influence of current density on removal yield under steady state conditions.

did not modify significantly the liquid recirculation velocity measured in batch conditions, about 0.2 cm/s in the riser. We used the assumption that the operation could be transposed to continuous flow condition if the residence time was higher than the operation time needed for batch conditions. To reach more rapidly steady state conditions, the reactor was filled with water with the same fluoride content as the inlet stream. To test the robustness of this assumption, drastic conditions were studied: a high initial fluoride content stream $[F^-]_0 = 20$ mg/L and pH 7 that is not the optimum value.

Experimental results using the same geometry as in batch conditions ($H_1 = 58$, $h = 14$ cm) showed that complete flotation was obtained, as expected. Fig. 8a confirms that $[F^-]$ tended to a plateau value beyond 17 min, this value being nearly independent of j, as expected for a circulation time of about 3 min. Using the zero-order constant defined by Eq. (10), the kinetic model deduced from batch process predicts a minimum current density of 20 mA/cm^2 for a residence time of 20 min to achieve the objective. Although this kinetic model did not apply for low $[F^-]$ values (Fig. 4), Fig. 8b shows that this rough estimation is in good agreement with experimental data under continuous flow conditions, which is promising for future applications to treatment of drinking water. Fig. 8b highlights also the key role of current density as a control parameter of the EC process.

Now, further research is still required. First, it seems necessary to better analyze the influence of other parts of the geometry of the airlift reactor (especially the separator section). Then, the kinetic model must be refined in order to optimize the defluoridation process and to establish a robust procedure to transpose EC from batch to continuous operation.

5. Conclusions

As a conclusion, this work has demonstrated that external-loop airlift reactors can be suitable EC cells in which complete flotation can be achieved using only electrochemically generated hydrogen microbubbles without the need for surfactants to induce the overall liquid recirculation. A fluoride concentration lower than 1.5 mg/L could always be achieved when initial F^- concentration was between 10 and 20 mg/L. The effects of conductivity and pH were in accordance with those reported in the literature. Conversely, the low electrode surface vs. reactor volume ratio that characterized the airlift reactor combined the advantages of conventional EC cells and chemical coagulation units: i.e. the formation of fluoroaluminum microflocs easy to flocculate near the electrodes to fluoride adsorption on these particles in the riser and the separator sections. This resulted in higher F/Al ratio in sludge at the expense of direct F^- attachment on the electrodes, which differed widely from conventional EC cells. As a result, fluoride removal could be achieved both at lower energy and lower electrode consumptions than in the literature on EC. The methodology used in this work allowed the definition of optimum EC conditions, $j = 6$ mA/cm^2 at pH 5, that accounted simultaneously for mixing, removal yield, reaction time and operating costs. Another advantage of the airlift reactor is that flocs were recovered only by flotation, which avoids the need for a downstream settling step. Exploratory experiments using continuous EC operation were also promising for future application to drinking water treatment: steady state conditions could be predicted using data from batch experiments, which shows that the transposition from batch to continuous operation seems easy.

References

[1] WHO, World health Organization: Fluoride in drinking water, WHO guidelines for drinking water quality (3 April 2005), 2004 http://www.who.int/water_sanitation_health/dwq/chemicals/fluoride.pdf.
[2] J. Qian, A.K. Susheela, A. Mudgal, G. Keast, Fluoride in water: an overview, Unicef Publication on Water, Environment Sanitation and Hygiene 13 (1999) 11–13.
[3] E.J. Readron, Y. Wang, A limestone reactor for fluoride removal from wastewaters, Environmental Science and Technology 34 (2000) 3247–3253.
[4] C.Y. Hu, S.L. Lo, W.H. Kuan, Y.D. Lee, Removal of fluoride from semiconductor wastewater by electrocoagulation–flotation, Water Research 39 (2005) 895–901.
[5] C.Y. Hu, S.L. Lo, W.H. Kuan, Effects of the molar ratio of hydroxide and fluoride to Al(III) on fluoride removal by coagulation and electrocoagulation, Journal of Colloid and Interface Science 283 (2005) 472–476.
[6] C. Castel, M. Schweizer, M.O. Simonnot, M. Sardin, Selective removal of fluoride ions by a two-way ion-exchange cyclic process, Chemical Engineering Science 55 (2000) 3341–3352.
[7] H. Luocini, L. Addour, D. Belhocine, H. Grib, S. Nicolas, B. Barion, N. Mameri, Study of new technique for fluoride removal from water, Desalination 114 (1997) 241–251.
[8] X. Fan, D.J. Parker, M.D. Smith, Adsorption kinetics of fluoride on low cost materials, Water Research 37 (2003) 4929–4937.
[9] V.K. Gupa, I. Ali, V.K. Saini, Defluoridation of wastewaters using waste carbon slurry, Water Research 41 (2007) 3307–3316.
[10] V. Gopal, K.P. Elango, Equilibrium, kinetic and thermodynamic studies of adsorption of fluoride onto plaster of Paris, Journal of Hazardous Materials 141 (2007) 98–105.
[11] W. Nigussie, F. Zewge, B.S. Chandravanshi, Removal of excess fluoride from water using waste residue from alum manufacturing process, Journal of Hazardous Materials 147 (2007) 954–963.
[12] Z. Amor, S. Malki, M. Taky, B. Bariou, N. Mameri, A. Elmidaoui, Optimization of fluoride removal from brackish water by electrodialysis, Desalination 120 (1998) 263–271.
[13] Z. Amor, B. Bariou, N. Mameri, M. Taky, S. Nicolas, A. Elmidaoui, Fluoride removal Corn brackish water by electrodialysis, Desalination 133 (2001) 215–223.

[14] M. Tahaikt, R. El Habbani, A. Ait Haddou, I. Achary, Z. Amor, M. Taky, A. Alami, A. Boughriba, M. Hafsi, A. Elmidaoui, Fluoride removal from groundwater by nanofiltration, Desalination 212 (2007) 46–53.
[15] Meenakshi, R.C. Maheshwari, Fluoride in drinking water and its removal, Journal of Hazardous Materials B137 (2006) 456–463.
[16] N. Mameri, A.R. Yeddou, H. Lounici, D. Belhocine, H. Grib, B. Bariou, Defluoridation of septentrional Sahara water of North Africa by electrocoagulation process using bipolar aluminium electrodes, Water Research 32 (1998) 1604–1612.
[17] N. Mameri, H. Lounici, D. Belhocine, H. Grib, D.L. Piron, Y. Yahiat, Defluoridation of Sahara water by small plant electrocoagulation using bipolar aluminium electrodes, Separation Purification Technology 24 (2001) 113–119.
[18] C.Y. Hu, S.L. Lo, W.H. Kuan, Effects of co-existing anions on fluoride removal in electrocoagulation (EC) process using aluminum electrodes, Water Research 37 (2003) 4513–5452.
[19] F. Shen, X. Chen, P. Gao, G. Chen, Electrochemical removal of fluoride ions from industrial wastewater, Chemical Engineering Science 58 (2003) 987–993.
[20] J. Zhu, H. Zhao, J. Ni, Fluoride distribution in electrocoagulation defluoridation process, Separation and Purification Technology 56 (2007) 184–191.
[21] P.K. Holt, G.W. Barton, C.A. Mitchell, The future for electrocoagulation as a localised water treatment technology, Chemosphere 59 (2005) 355–367.
[22] M.Y.A. Mollah, R. Schennach, J. Parga, D.L. Cocke, Ectrocoagulation (EC)—science and applications, Journal of Hazardous Materials 84 (2001) 29–41.
[23] M.Y.A. Mollah, P. Morkovsky, J.A.G. Gomes, M. Kesmez, J. Parga, D.L. Cocke, Fundamentals, present and future perspectives of electrocoagulation, Journal of Hazardous Materials 114 (2004) 199–210.
[24] Y. Chisti, Airlift Bioreactors, Elsevier, London, 1989.
[25] J.B. Joshi, V.V. Ranade, S.D. Gharat, S.S. Lele, Sparged-loop reactors, Canadian Journal of Chemical Engineering 68 (1990) 705–741.
[26] X. Chen, G. Chen, P.L. Yue, Investigation on the electrolysis voltage of electrocoagulation, Chemical Engineering Science 57 (2002) 2449–2455.
[27] M. Khemis, J.P. Leclerc, G. Tanguy, G. Valentin, F. Lapicque, Treatment of industrial liquid wastes by electrocoagulation: experimental investigations and an overall interpretation model, Chemical Engineering Science 61 (2006) 3602–3609.
[28] A.H. Essadki, M. Bennajah, B. Gourich, Ch. Vial, M. Azzi, H. Delmas, Electrocoagulation/electroflotation in an external-loop airlift reactor - Application to the decolorization of textile dye wastewater, Chemical Engineering and Processing: Process Intensification 47 (2008) 1211–1223.
[29] Y. Chisti, M. Moo-Young, Airlift reactors: applications and design considerations, Chemical Engineering Science 43 (1987) 451–457.
[30] R.A. Bello, A characterization study of airlift contactors for applications to fermentations, PhD Thesis, University of Waterloo, Ontario, Canada, 1981.
[31] K.H. Choi, W.K. Lee, Circulation liquid velocity, gas holdup and volumetric oxygen transfer coefficient in external-loop airlift reactors, Journal of Chemical Technology & Biotechnology 56 (1993) 51–58.
[32] M.M. Emamjomeh, M. Sivakumar, An empirical model for defluoridation by batch monopolar electrocoagulation/flotation (ECF) process, Journal of Hazardous Materials B131 (2006) 118–125.
[33] C.Y. Hu, S.L. Lo, W.H. Kuan, Simulation the kinetics of fluoride removal by electrocoagulation (EC) process using aluminium electrodes, Journal of Hazardous Materials 145 (2007) 180–185.
[34] L. Sánchez Calvo, J.P. Leclerc, G. Tanguy, M.C. Cames, G. Paternotte, G. Valentin, A. Rostan, F. Lapicque, An electrocoagulation unit for the purification of soluble oil wastes of high COD, Environmental Progress 22 (2003) 57–65.